International Journal of Business, Human and Social Sciences
ISSN: 2517-9411
Vol:10, No:4, 2016

Performance Analysis of New Types of Reference Targets Based on Spaceborne and Airborne SAR Data

Y. S. Zhou, C. R. Li, L. L. Tang, C. X. Gao, D. J. Wang, Y. Y. Guo

***Abstract*—**Triangular trihedral corner reflector (CR) has been widely used as point target for synthetic aperture radar (SAR) calibration and image quality assessment. The additional "tip" of the triangular plate does not contribute to the reflector's theoretical RCS and if it interacts with a perfectly reflecting ground plane, it will yield an increase of RCS at the radar bore-sight and decrease the accuracy of SAR calibration and image quality assessment. Regarding this problem, two types of CRs were manufactured. One was the hexagonal trihedral CR. It is a self-illuminating CR with relatively small plate edge length, while large edge length usually introduces unexpected edge diffraction error. The other was the triangular trihedral CR with extended bottom plate which considers the effect of 'tip' into the total RCS. In order to assess the performance of the two types of new CRs, flight campaign over the National Calibration and Validation Site for High Resolution Remote Sensors was carried out. Six hexagonal trihedral CRs and two bottom-extended trihedral CRs, as well as several traditional triangular trihedral CRs, were deployed. KOMPSAT-5 X-band SAR image was acquired for the performance analysis of the hexagonal trihedral CRs. C-band airborne SAR images were acquired for the performance analysis of the bottom-extended trihedral CRs. The analysis results showed that the impulse response function of both the hexagonal trihedral CRs and bottom-extended trihedral CRs were much closer to the ideal sinc-function than the traditional triangular trihedral CRs. The flight campaign results validated the advantages of new types of CRs and they might be useful in the future SAR calibration mission.

***Keywords*—**Synthetic Aperture Radar, calibration, corner reflector, KOMPSAT-5.

I. Introduction

SYNTHETIC Aperture Radar (SAR) calibration is becoming much important than ever before due to the increasing image resolution and demand of quantitative remote sensing applications [1]. The trihedral CR is one of the most important types of reference targets for SAR radiometric/geometric calibration and image quality assessment [2], [3].

The geometry of the reflection plate of the trihedral CR is traditionally chosen to be triangular. The additional "tip" of the triangular plate has no contribution to the reflector's theoretical radar cross-section (RCS) and thus if it interacts with a perfectly reflecting ground plane, it will influence the backscatterering signal of the CR and make the SAR calibration and image quality assessment approach unreliable [4].

For this problem, some advanced CRs were developed. On the one hand, the concept of self-illuminating CR was proposed [4], where self-illuminating means that all the rays that enter the reflector's cavity experience the triple reflection on the panel and return to the radar. Furthermore, since the unexpected plate edge diffraction is proportional to the plate edge length, the panel geometry was assumed as polygon, and optimum hexagonal panel geometry was obtained while minimizing the edge length, i.e., $1.9441\sqrt{s}$ (where $\sqrt{s}$ indicates reflector panel's area). Because the circle has the shortest perimeter among all planar shapes with the same area, CR plate with curve edge was proposed and the minimal edge was further reduced to $1.9282\sqrt{s}$ [5], [6]. On the other hand, the triangular trihedral CR with extended bottom plate was proposed, which included the contribution of extended bottom to the total RCS [7].

For assessing the performance of the two types of advanced CRs, six hexagonal trihedral CRs, two bottom-extended trihedral CRs, as well as traditional triangular trihedral CRs, were deployed at the National Calibration and Validation Site for High Resolution Remote Sensors. The C-band airborne SAR image and X-band spaceborne KOMPSAT-5 SAR image were acquired for the performance analysis.

The rest of the paper is organized as follows. In Section II, the two types of CRs will be introduced, while simulation results will be presented to show the performance the CRs. The flight experiment will be described in Section III. In Section IV, the acquired airborne and spaceborne SAR data will be shown and the performance of CRs will be analyzed. Finally, conclusions are drawn in Section V.

II. New Types of Corner Reflectors

The triangular trihedral CR has the advantages of large peak RCS, extremely wide RCS pattern, light weight, cheap and simple to manufacture. The panel geometry for the trihedral CR has been traditionally chosen as triangular shape. However, as shown in Fig. 1, not all the panel area is the effective area which contributes to the nominal RCS $\sigma = 4\pi l^4/(3\lambda^2)$. The additional 'tip' reflecting area, if interacting with ground plane, will yield an increase of RCS. This problem will decrease SAR radiometric and phase calibration accuracy.

Y. S. Zhou is with the Key Lab of Quantitative Remote Sensing Information Technology, Academy of Opto-Electronics, Chinese Academy of Sciences, Beijing, China (phone: +86-10-82178646; fax: 86-10-82178600; e-mail: zhouys@aoe.ac.cn).

C. R. Li, L. L. Tang, and C. X. Gao are with the Key Lab of Quantitative Remote Sensing Information Technology, Academy of Opto-Electronics, Chinese Academy of Sciences, Beijing, China (e-mail: crli@aoe.ac.cn, lltang@aoe.ac.cn, gaocaixia@aoe.ac.cn).

D. J. Wang and Y. Y. Guo are with the Key Laboratory of Electromagnetic Space Information, University of Science and Technology of China, Hefei, China (e-mail: wangdj@ustc.edu.cn, yuanyueg@ustc.edu.cn).

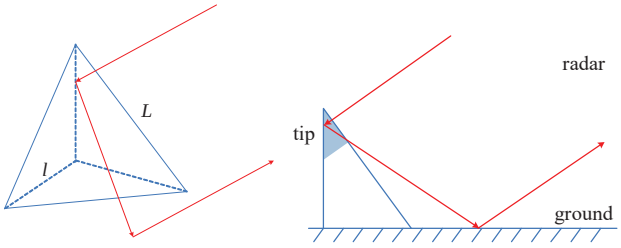

(a) 3-D view (b) lateral view

Fig. 1 The effect of additional 'tip' reflecting area on reflection

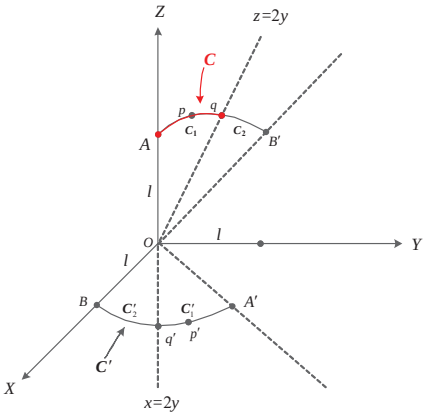

Fig. 2 Geometry of a self-illuminating trihedral CR

A. Self-Illuminating Trihedral Corner Reflectors [4]-[6]

The self-illuminating trihedral CR was proposed to solve the problem. Fig. 2 shows the geometry of a self-illuminating trihedral CR.

Let curve $\boldsymbol{C}$ has the following parameterized form:

$$\boldsymbol{C}(\tau) = [0,\ f(\tau),\ g(\tau)], \qquad \tau \in [0, t] \tag{1}$$

According to the property of self-illuminating trihedral CR, the area of one panel of the self-illuminating trihedral CR could be expressed by

$$S = 2 \cdot \int_0^{t_0} \left(f_1' g_1 - g_1' f_1 \right) d\tau \tag{2}$$

where f' denotes the partial derivatives of f, and g' denotes the partial derivatives of g. The edge length of the self-illuminating trihedral CR is then expressed by

$$L = 2 \cdot \int_0^{t_0} \left\{ \sqrt{f_1'^2 + g_1'^2} + \sqrt{(f_1' - g_1')^2 + g_1'^2} \right\} d\tau \tag{3}$$

The purpose of the optimization is to choose f so that it would minimize (3) subject to the constraint of (2).

If the curve $\boldsymbol{C}$ is specially assumed to be straight line, i.e., the geometry is polygon, the hexagon is the optimal shape which has the minimal edge length for the same panel area, as shown in Table I. If the curve $\boldsymbol{C}$ is specially assumed to be circular arc, an optimal geometry will be derived while the edge length could be further reduced.

TABLE I
COMPARISON OF THE EDGE LENGTHS OF DIFFERENT PANEL GEOMETRIES

Edge Types	straight line			circular arc	ellipse edge
	square	pentagon	hexagon		
Panel area	S	S	S	S	S
Interior leg length	$\sqrt{S}$	$0.866\sqrt{S}$	$0.9469\sqrt{S}$	$0.932\sqrt{S}$	$0.932\sqrt{S}$
Minimum of external edge length	$2\sqrt{S}$	$2.1\sqrt{S}$	$1.9441\sqrt{S}$	$1.9282\sqrt{S}$	$1.9282\sqrt{S}$

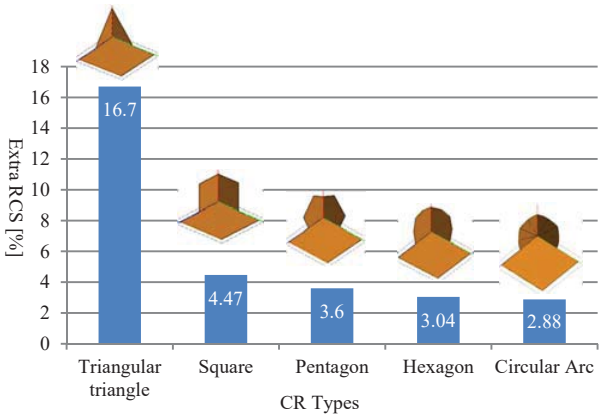

Fig. 3 The effect of ground on total RCS of various CRs

Fig. 3 shows the effect of ground on total RCS of various types of CRs through the RCS simulation method. The isosceles triangular trihedral CR is mostly affected by the ground, while the hexagonal and circular-arc trihedral CRs are less affected. In practice, hexagonal trihedral CRs have been manufactured due to their simplicity in geometry.

B. Bottom-Extended Trihedral Corner Reflectors [7]

Trihedral CR with extended bottom plate includes the effect of the additional 'tip' reflecting area in the total RCS. In order to ensure all the rays that enter into the CR can be reflected back to the radar, the bottom length X should satisfy the following equation:

$$X \geq l \tan\theta \tag{4}$$

In practice, two bottom-extended trihedral CRs with l =0.8m

and X =1.36m had been manufactured for the incidence angle of 59.5° .

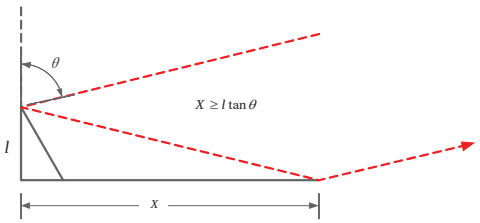

Fig. 4 Geometry of the bottom-extended trihedral CR

III. Flight Experiments

A. Airborne SAR Experiments for the Performance Analysis of Bottom-Extended Trihedral CR

In order to analyze the performance of the bottom-extended trihedral CRs, two of them and several triangular trihedral CRs were deployed at the National Calibration and Validation Site for High Resolution Remote Sensors.

Fig. 5 The bottom-extended trihedral CR deployed in the National Calibration and Validation Site for High Resolution Remote Sensors

Table II shows the airborne SAR parameters.

TABLE II
Airborne SAR Data Parameters

Parameters	Value
Center frequency	5.5 GHz (C-band)
High resolution mode imagery	0.6m
Processing band width	250MHz
Polarization	HH
Beam width	6°
NESZ	≤ -25 dB
Central incidence angle	60°

Since the central incident angle is 60°, as shown in Fig. 6, the tilted angel should be adjusted to be $-2.74°$, which means that the CR should be tilted forward to ground and thus the ground will have great effect on the radar backscatterering power.

B. Spaceborne SAR Experiments for the Performance Analysis of Hexagonal Trihedral CR

In order to analyze the performance of the hexagonal trihedral CRs, six hexagonal trihedral CRs and one triangular trihedral CR were deployed at the National Calibration and Validation Site for High Resolution Remote Sensors.

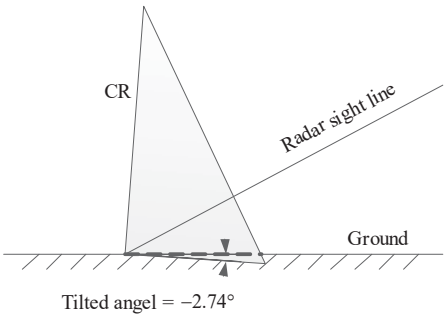

Fig. 6 Illustration of the CR deployment

(a) deployment array (b) the deployed CR

Fig. 7 The hexagonal trihedral CR deployed in the National Calibration and Validation Site for High Resolution Remote Sensors

Table III shows the spaceborne SAR parameters.

TABLE III
Kompsat-5 Data Parameters

Parameters	Value
Center frequency	9.66 GHz (X-band)
High resolution mode imagery	1 m GSD, 5 km swath width
Polarization	HH
NESZ (Noise Equivalent Sigma Zero)	≤ -17 dB
Orbit direction	Descending
Beam ID	HR-22
Far incidence angle	45.932867886597322°
Near incidence angle	45.597960269190473°

IV. CR Performance Analysis

A. Performance Analysis of Bottom-Extended Trihedral CR

The C-band airborne SAR images of the two bottom-extended trihedral CRs and two triangular trihedral CRs are shown in Figs. 8 (a) and (b), respectively. The 2-D point shape of the bottom-extended trihedral CR is much closer to the ideal "+" shape than the traditional triangular trihedral CR. In other words, the effect of the ground on the bottom-extended trihedral CR is less than the traditional triangular CR.

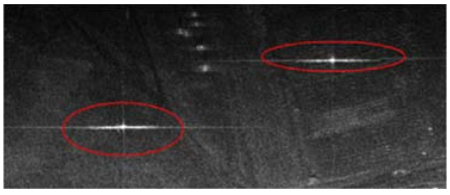

(a) Bottom-extended trihedral CRs

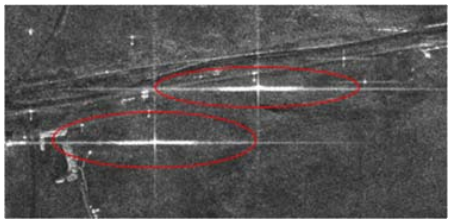

(b) Triangular trihedral CRs

Fig. 8 C-band airborne SAR images

B. Performance Analysis of Hexagonal Trihedral CR

The spaceborne SAR image of the six hexagonal trihedral CRs and one triangular trihedral CR is shown in Fig. 9. Both the 2-D point shapes of the hexagonal trihedral CRs and the triangular trihedral CR are closer to the ideal "+" shape.

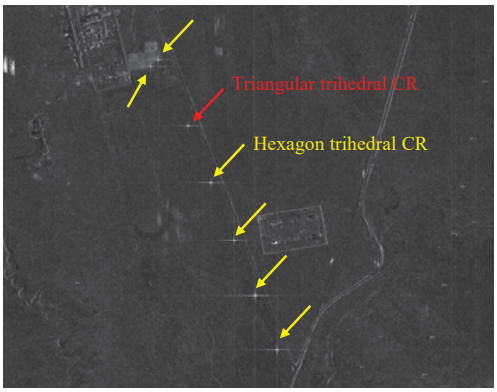

Fig. 9 X-band spaceborne KOMPSAT-5 SAR image of the deployed CRs

The range and azimuth 1-D data profiles of the hexagonal trihedral CR and the triangular trihedral CR are shown in Figs. 11 and 12, respectively. It shows that the azimuth 1-D impulse response function of the hexagonal trihedral CR is much closer to the ideal form (cf. Fig. 10) than that of the traditional triangular trihedral CR.

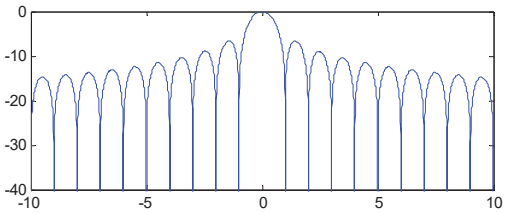

Fig. 10 Illustration of the ideal point response function

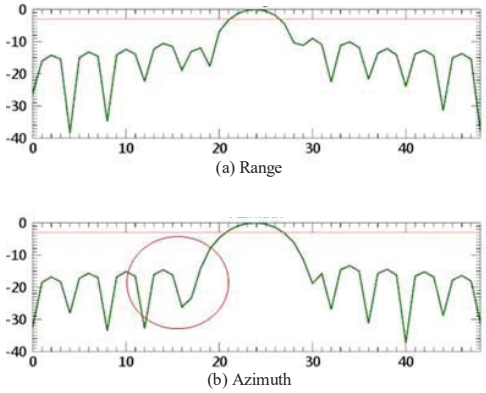

(a) Range

(b) Azimuth

Fig. 11 Range and azimuth 1-D impulse response functions of a hexagonal trihedral CR

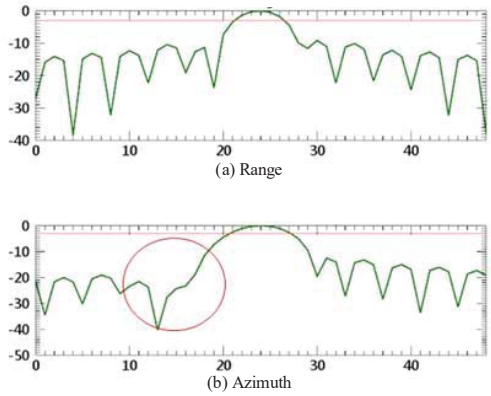

(a) Range

(b) Azimuth

Fig. 12 Range and azimuth 1-D impulse response functions of the triangular trihedral CR

V. Conclusion

The performance of SAR calibration and image quality assessment based on traditional trihedral CRs are easily affected by the ground-tip interaction. This paper preliminarily analyzed the effectiveness of two types of advanced CRs through airborne SAR data and spaceborne SAR data. The results show that the 2D and azimuth 1D impulse response functions are much closer to the ideal function, which will make the CR more practical and improve the calibration and image quality assessment accuracy. In the future, quantitative analysis on the performance improvement in radiometric calibration will be carried out.

Acknowledgment

This work was supported in part by the National High Technology Research and Development Program of China (Grant No. 2013AA122903, 2013AA122102), and in part by the National Natural Science Foundation of China (Grant No. 61331020, 61571422, 51409143).

References

[1] Y. S. Zhou, W. Hong, Y. P. Wang, and Y. R. Wu, "Maximal effective baseline for polarimetric interferometric SAR forest height estimation,"

Science China Information Sciences, vol. 55, no. 4, pp. 867-876, 2012.
[2] A. Freeman, "SAR calibration: An overview," *IEEE Transactions on Geoscience and Remote Sensing*, vol. 30, no. 6, pp. 1107-1121, Nov. 1992.
[3] A. W. Doerry, "Reflectors for SAR Performance Testing," Sandia National Laboratories 2008.
[4] K. Sarabandi and T. C. Chiu, "Optimum corner reflectors for calibration of imaging radars," *IEEE Transactions on Geoscience and Remote Sensing*, vol. 44, no. 10, pp. 1348-1361, 1996.
[5] C. R. Li, Y. S. Zhou and L. L. Ma, "Analysis of Optimal Panel Geometry for Self-Illustration Corner Reflector," in *Proc. Progress in Electromagnetics Research Symposium*, Guangzhou, China, pp. 1425-1429.
[6] Y. S. Zhou, C. R. Li, L. L. Ma, M. Y. Yang, and Q. Liu, "Improved trihedral corner reflector for high-precision SAR calibration and validation," in *Proc. 2014 IEEE International Geoscience and Remote Sensing Symposium*, Quebec, Canada, 2014, pp. 454-457.
[7] A. W. Doerry and B. C. Brock, "Radar Cross Section of Triangular Trihedral Reflector with Extended Bottom Plate," Sandia National Laboratories 2009.